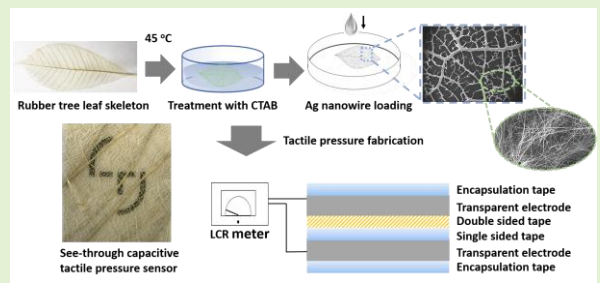


Biodegradable, Flexible and Transparent Tactile Pressure Sensor Based on Rubber Leaf Skeletons

Anastasia Koivikko, Vilma Lampinen, Kyriacos Yiannacou, Vipul Sharma* and Veikko Sariola*, *Member IEEE*

Abstract— Capacitive sensors have many applications in tactile sensing, human-machine interfaces, on-body sensors, and patient monitoring. Particularly in biomedical applications, it would be beneficial if the sensor is disposable and readily degradable for efficient recycling. In this study, we report a biodegradable capacitive tactile pressure sensor based on sustainable and bio resourced materials. Silver-nanowire-coated rubber tree leaf skeletons are used as transparent and flexible electrodes while a biodegradable clear tape is used as the dielectric layer. The fabricated sensor is sensitive and can respond to low pressures (7.9 mN when pressed with a probe with a surface area of 79 mm² / 0.1 kPa) ranging to relatively high pressures (37 kPa), with a sensitivity up to $\approx 4.5 \times 10^{-3}$ kPa⁻¹. Owing to all bio resourced constituents, the sensor is biodegradable and does not create electronic waste.



Index Terms— Bioinspiration; capacitive sensors; leaf skeleton; Ag nanowires

I. INTRODUCTION

FLEXIBLE devices are intensively researched [1], [2], due to their promising applications in flexible displays [3], flexible sensors [4], flexible solar cells [5], artificial electronic skins (“e-skins”) [6], human-computer interfaces [7], and many other devices [8]–[10]. As the applications of electronic devices are increasing, so is the waste created by disposed electronic devices (electronic waste, e-waste). E-waste is posing a serious threat to the environment [11]. To limit the growing amount of e-waste, it would be highly preferable to have the devices disposable and easily recyclable: for example, by having it degradable and decomposable, just like most nature-derived materials.

Among the many applications of flexible devices, tactile pressure sensors, or touch detectors play an essential role [12], [13]. For tactile pressure sensors, the capacitive sensing principle has been widely used [14], [15]. A capacitive tactile pressure sensor consists of two conductive electrodes, with a dielectric in between. An ideal electrode material has low cost, low resistance, and high flexibility. Furthermore, high optical transmittance is needed for some applications e.g. transparent electronic skins.

Extensive research has been conducted to assess the potential of paper and eco-friendly polymer-based electronics and proof of concept touch sensors have been demonstrated using such materials [16]–[18]. These paper and polymer-based touch sensors are fabricated in cleanrooms, using sophisticated techniques such as photolithography and physical vapor deposition. These facilities and processes are very expensive, despite the cheap cost of the paper or the polymer substrate itself. Apart from high costs, such fabrication processes involve

the use and disposal of many chemicals which are harmful to the environment. Studies are claiming that relatively easier fabrication on paper and polymer substrates can be achieved by using Ag nanowire inks and other nanocomposites [18]–[20]. However, efforts to improve the transparency and the performance of sensors based on Ag nanowires are still being pursued.

In this study, we report the fabrication of capacitive pressure sensors out of plant-based materials. A skeleton of rubber tree leaf (*Hevea brasiliensis*), coated with Ag nanowires, was used as a transparent and flexible electrode (Fig. 1a) while a biodegradable cellulose clear tape was used as a dielectric layer. The electrode was fabricated by dispersing Ag nanowires on the leaf skeleton. The skeleton has an interconnected fractal-like structure, composed of lignin and other biomaterials. The interconnected fractal-like design provides stability and good surface coverage with a small amount of material. This fractal-like architecture is responsible for high flexibility and allows the repeated bending of the surface. Skeleton of the rubber tree leaf was used as it is very flexible, provides decent transparency, is not fragile, and is readily available. It is also noteworthy to mention that the leaf skeletons of rubber tree leaf used in this study are not the only natural surfaces that can be used as electrodes. Many leaf skeletons display unique fractal architectures at different length scales. Ag nanowire coating can be done to any type of leaves that can be skeletonized and provide freestanding fractal structures [21], [22]. The biodegradable tape provides layered structures with adhesive and air gaps. These layers act as a compressible architecture, elastically collapsing under pressure. The fabricated sensor was sensitive (4.5×10^{-3} kPa⁻¹) and responded to a variety of pressure ranges (0.1 – 37 kPa). This strategy of directly using plant-

based materials for the fabrication of capacitive sensors will provide valuable insights towards a sustainable, scalable, and facile approach to fabricate flexible electronics.

II. MATERIALS AND METHODS

A. Materials

For the fabrication of the leaf skeleton electrode, leaf skeletons of *Hevea brasiliensis* were purchased from skeleton-leaf.com (United Kingdom). Ag-nanowires (diameter: 30 nm, Length: 20-50 μm) in ethanol and cetrimonium bromide (CTAB), were purchased from Merck, Finland. All the chemicals were used as received. Cellulose clear tape was purchased from Shurtape (USA).

B. Fabrication of leaf skeleton electrode and capacitive sensor

First, the leaf skeletons were dipped in 1mM solution of CTAB in DI water (ELGA purelab) and dried overnight at room temperature. Next, the leaf skeletons were placed inside hydrophobic Petri dishes, along with Ag nanowires (150 mg cm^{-2} , diluted in ethanol + water in 1:1 ratio), and allowed to dry under ambient conditions for 1 h. Finally, the skeletons were placed over a hot plate and dried for 30 min at 100 $^{\circ}\text{C}$.

For the fabrication of the capacitive sensor, rubber leaf skeleton electrodes were used as the top and the bottom electrodes of the capacitor. A single-sided cellulose clear tape was applied to the bottom side of the upper electrode. Double-sided tape was used to connect the bottom electrode to the top electrode. The sensor was sealed with the cellulose clear tape applied on the two exposed sides of the electrodes. Finally, the wires were attached to the sensor by crimping them (10025-12, Nicomatic). The schematic of the fabrication and structure of the rubber leaf skeleton-based transparent electrode and the capacitive sensor is illustrated is shown in Figs. 1a and b, respectively.

C. Characterization methods

High-resolution surface structure characterization was performed by using an SEM (scanning electron microscope) (Jeol IT-500) operating at 5 kV. The elemental mapping of the leaf was done using an EDS (Energy-dispersive X-ray spectroscopy) attachment linked to SEM (JEOL). The sheet resistance of the skeleton leaf surfaces was measured using a general-purpose multimeter. Ag nanowire coated leaf skeletons of size 3 cm \times 3 cm were cut and a copper tape (3M) was applied to the opposite sides of the before the resistance was measured.

The fabricated sensors were characterized by using a mechanical tester (TA.XT Plus, Stable Micro Systems) with a non-conducting cylindrical probe (\varnothing 10 mm) for producing varying pressure P . LCR meter (ST2827A, Sourcetrionics) was used to measure the corresponding capacitance C in the sensor.

III. RESULTS AND DISCUSSION

A. General Morphology

The morphology of the transparent electrode was investigated with SEM. The leaf skeleton shows fractal-like interconnected veins at the microscale (Figs. 2a and b). This framework provides support to the Ag nanowires which formed

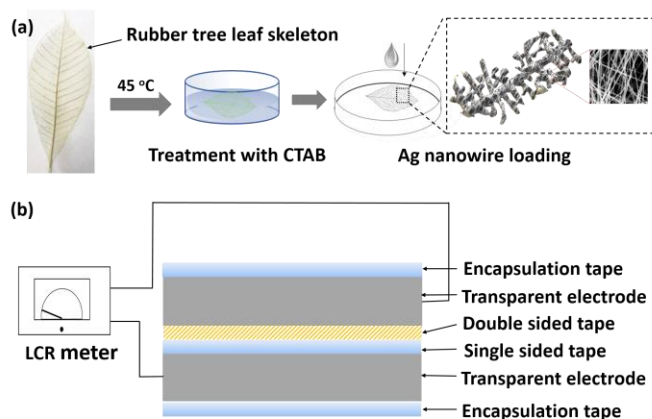


Fig.1. Fabrication of the biodegradable sensor. a) Schematic of the fabrication of transparent electrode. b) The layout of the biodegradable capacitive sensor, including leaf electrodes, dielectric tapes, and encapsulation tapes.

a conductive network across the skeleton (Fig. 2c). The scanning electron micrographs show a network of Ag nanowire of length \sim 20 – 50 μm spread across the skeleton surfaces. The nanowires are evenly spread and conformally adhered to the surface to form a continuous nano-network throughout the area. The vascular bundles along with the interconnected fibers of the leaf skeleton can be seen in the SEM images. The cross-sectional image (Fig. 2d) shows the layers of the sensors where the dielectric layer composed of tape (including adhesive material), leaf electrodes, and the encapsulating tape layers are evident.

To confirm the even distribution of the Ag nanowires on the rubber leaf skeleton surface, the EDS measurements were done. The EDS mapping data corresponding to the SEM images is shown in Fig. 3 which confirms the presence of Ag nanowires evenly distributed across the surface of the leaf skeleton. The elements C, N, O and K are also evident which are main constituents of the leaf skeleton.

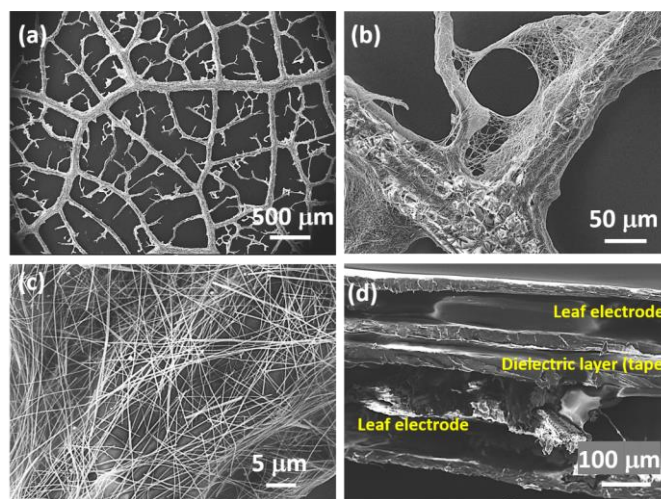


Fig. 2. a-c) SEM images of rubber leaf skeletons coated with Ag nanowires. d) Scanning electron microscopy image displaying a cross-section of the sensor.

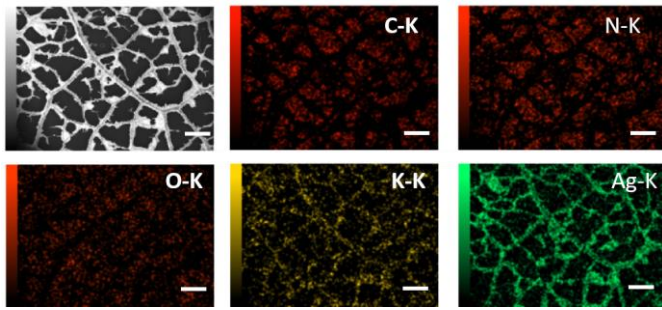


Fig. 3. EDS mapping of the Rubber leaf skeleton after deposition of Ag nanowires. Uniform coverage of the Ag nanowires on the surface is evident. The scalebar in all the images is 500 μm .

B. Resistance of the electrode

Bending can change the sheet resistance of the electrodes, which is undesirable. The conductivity of the rubber leaf skeleton electrode was measured using a general-purpose multimeter. To demonstrate the flexibility of the electrodes, the leaf electrode was clamped from its edges and bent with the help of a linear translation stage. Fig. 4a shows the conductivity of the leaf electrode where the skeleton electrode is used as a conductor in the circuit in a curved position to turn on an LED. The electrode had a sheet resistance of $<10 \Omega \text{sq}^{-1}$ (loading quantity of $\sim 150 \mu\text{g cm}^{-2}$ was used). The curvature of the leaf and the corresponding resistance were recorded as shown in Fig. 4b. The change in resistance value is almost negligible as the curvature is increased from 0 to 600 m^{-1} which shows the good flexibility of the leaf electrodes.

To check the stability of the electrode with respect to the change in temperature, we measured its resistance at different temperatures (Fig. 4c). The Ag nanowire coated leaf skeleton was placed on the hot plate, the temperature was ramped up in the interval of 15 $^{\circ}\text{C}$. The total time taken for the hot plate to reach 200 $^{\circ}\text{C}$ was ~ 11 min (~ 1 min per 15 $^{\circ}\text{C}$ step). The resistance values were recorded and plotted against the temperature intervals. The resistance was stable until 180 $^{\circ}\text{C}$. At temperatures above 180 $^{\circ}\text{C}$, the resistance increased substantially, which can be due to the snapping of the Ag nanowires at high temperatures [23].

C. Electrode transparency

To show the transparency of the rubber leaf skeleton electrode, transmittance measurements were done. Fig. 4d shows the relative transmittance spectra of the leaf skeleton electrode without tape, and with tape at visible and near-infrared wavelengths. The corresponding camera images are displayed in the inset. As evident from the figure, the relative optical transmittances of the electrode surfaces without and with tape (sheet resistances $\sim 10 \Omega \text{sq}^{-1}$) were in the range of 50 – 70%. The transmittance of the entire sensor displayed values of $\sim 20\%$, which is still decent to see through the sensor.

D. Mechanism

The sensing mechanism of the leaf skeleton and biodegradable tape-based leaf sensor is shown in Fig. 5. The sensor is essentially a plate capacitor, with capacitance C directly proportional to the area A of the electrodes, directly proportional to the permittivity ϵ of the dielectric layer, and inversely proportional to the distance d between the electrodes,

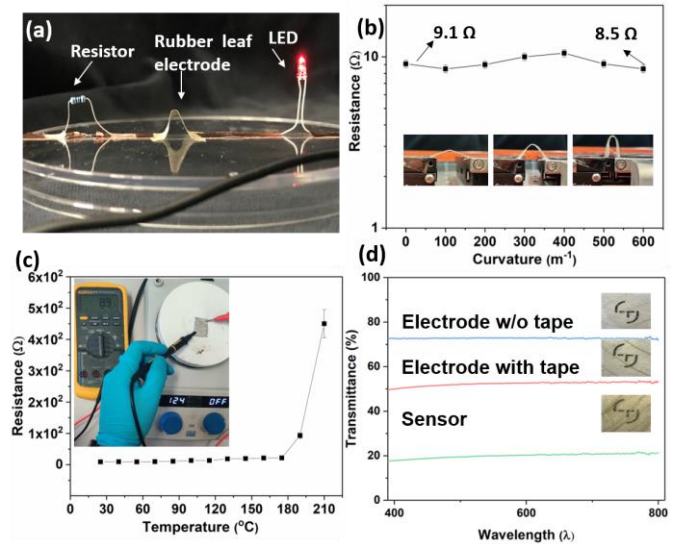


Fig. 4. (a) Photograph of the leaf skeleton electrode conducting electricity for powering an LED. (b) The change in resistance when the leaf skeleton electrode is bent. (c) The change in resistance when the leaf skeleton electrode is heated. (d) Relative transmittance spectra of the electrodes and the sensor.

i.e., $C \approx \epsilon A/d$. Any variation in A , ϵ , or d will lead to a variation in capacitance. For our sensors, the area $A \approx 2.25 \text{ cm}^2$ and d was estimated to be in the range of $\sim 300 - 400 \mu\text{m}$ (refer to Fig. 2d). When there is no load, the initial C is $\sim 10 - 12 \text{ pF}$ which increases up to 0.8 pF at a load of 40 kPa.

In Fig. 2d, the cross-sectional images of the double-sided and the single-sided tape shows that the dielectric layer consists of the adhesive with a very thin air film between the two tapes. The adhesive is pressure-sensitive, and rubber based (according to the specifications manufacturer) and it does not spread across the surfaces very conformally, especially at the interface of the adhesive–electrode. This provides hollow cavity-like structures or air pockets. The air pockets, the elastic nature of the adhesive and the electrodes make the sensor compressible. When the pressure is applied, d decreases mainly from the compression of the adhesive material and deformation of the air pockets.

The sensor provides high sensitivity even at very low pressures. The use of tapes as the dielectric layers offers an advantage over conventional dielectric layers as the adhesive material provides elasticity and offers a significant decrease in

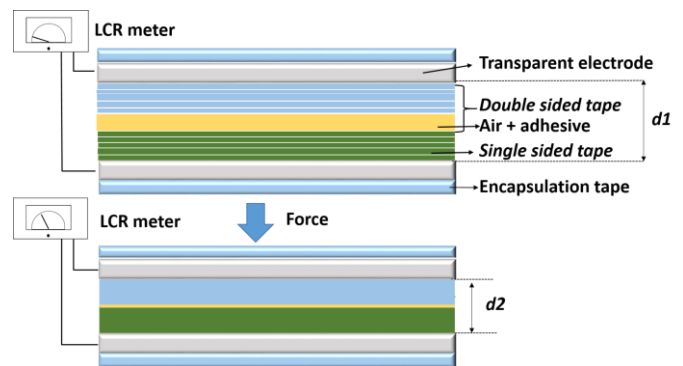


Fig. 5. Schematic of the capacitance sensing. The initial distance d_1 includes the double and single sided tapes and the air captured in the adhesive of the tapes. When the load is applied the distance d_2 is mainly caused by the double and single sided tapes.

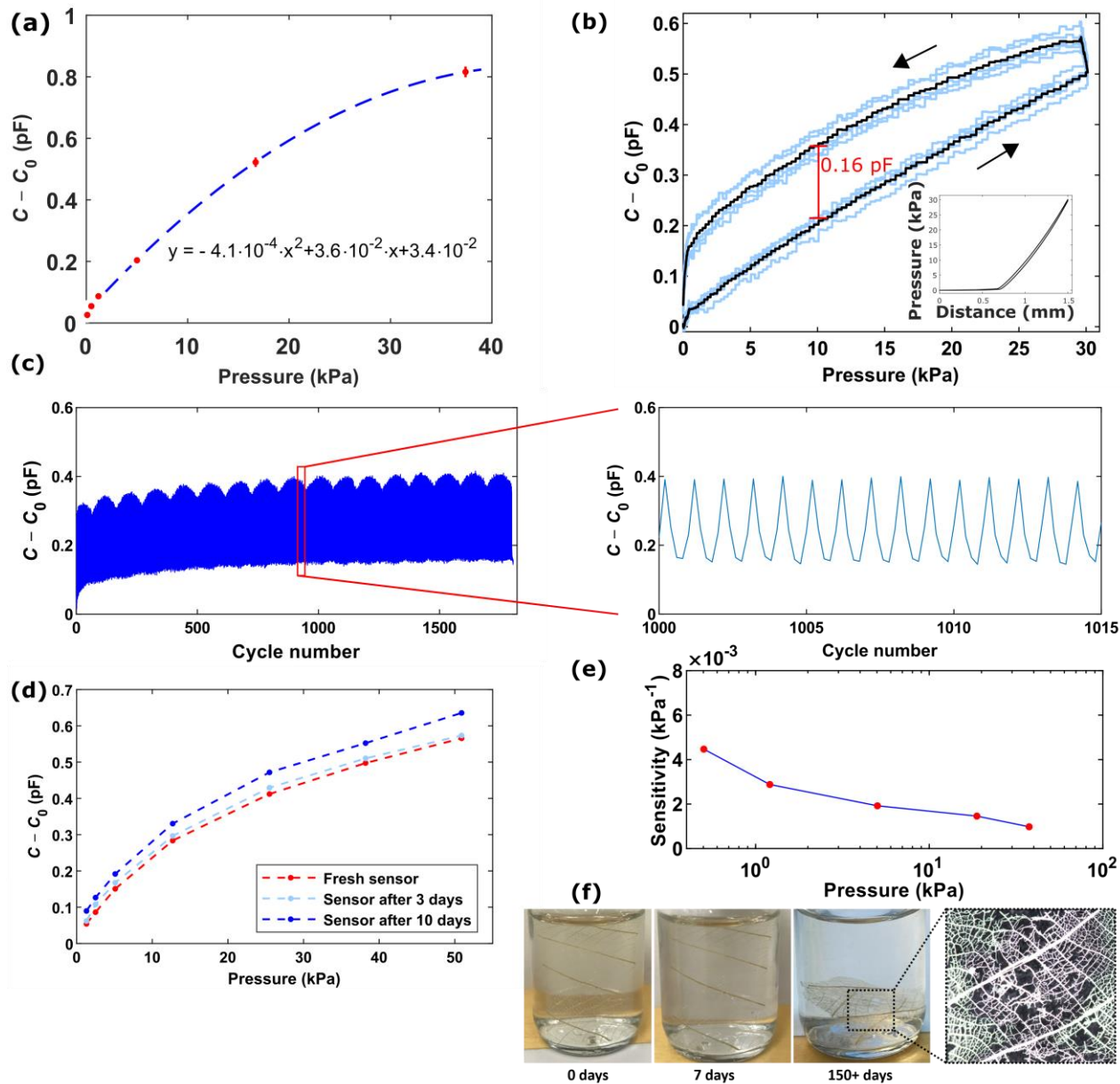


Fig. 6. Characterization of the capacitive sensor. a) Relative capacitance $C - C_0$ under varying applied pressure P , with fitted 2nd order polynomial. b) Hysteretic behavior of the sensor: $C - C_0$ versus 30 kPa load. Black graph is average of 5 repeats (blue graphs), the maximum hysteresis is 0.16 pF. The inset is the corresponding P - D curve from the measurements. c) Cyclic experiment with 1800 cycles of 12.5 kPa load and inset of 15 repeats. d) Relative C of the fresh sensor, 3 days old and 10 days old sensor versus the applied P . e) Sensitivity from the data in Fig. 6a). f) Degradation of the electrode in seven and over 150 days. Each point in the graphs indicates an average of five measurements, and error bars show standard deviation.

the thickness of the dielectric layer. Due to the presence of air pockets at the interface of the leaf electrode and adhesive-cellulose material of the tape, it is useful to think of the sensor as three capacitors in series, i.e., $C = 1/(1/C_{\text{air}} + 1/C_{\text{adhesive}} + 1/C_{\text{cellulose}}) = A/(d_{\text{air}}/\epsilon_{\text{air}} + d_{\text{adhesive}}/\epsilon_{\text{adhesive}} + d_{\text{cellulose}}/\epsilon_{\text{cellulose}})$. Due to the deformation of the air pockets, it is safe to assume that the variation in d_{air} is much larger than the variation in d_{adhesive} and $d_{\text{cellulose}}$. The dielectric constant of the cellulose is reported to be ~ 2.6 [24] and rubber is < 3 [25]. So we can assume that most of the variation in the capacitance arises from the variation in d_{air} [26], [27]. This explains why the elastically collapsible air pockets increase the sensitivity of the sensor.

E. Sensor Studies

The fabricated capacitive sensor was characterized by measuring relative capacitance $C - C_0$ under varying P in the range from 0.1 to 37.4 kPa (Fig. 6a). The pressure was applied stepwise by pressing the sensor with a cylindrical probe and then removing the pressure. Each pressure step was repeated five times and the peak values of the steps were captured. A second-order polynomial $y = -4.1 \cdot 10^{-4} \cdot x^2 + 3.6 \cdot 10^{-2} \cdot x + 3.3 \cdot 10^{-2}$ was fitted to the mean values.

Then, the hysteretic behavior of the sensor was studied by slowly and continuously loading and unloading the sensor five times. In these experiments, the maximum load was 30 kPa, and

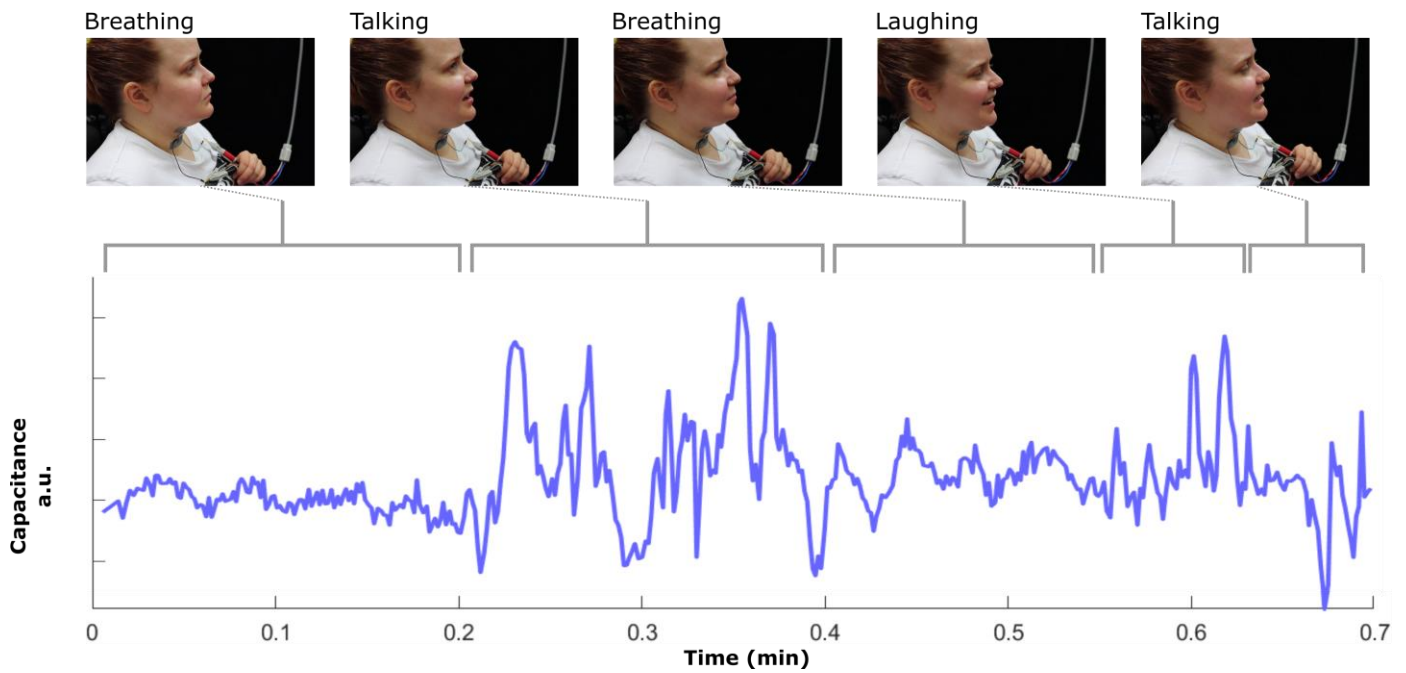


Fig. 7. Demonstration with the fabricated sensor. The sensor was attached in the middle of the neck of the test person and C was recorded while the test person breathing, speaking, and laughing.

it was held for 60 s. Fig. 6b shows the relative capacitance $C - C_0$ of the sensor versus the load P . The black graph is an average of five repeated measurements (blue graphs). The load decreased slightly from 30 kPa while the distance of the probe was kept constant during the 60 s hold, which can be caused by the geometric changes in the dielectric layer. The sensor had hysteretic behavior, the difference in the $C - C_0$, between the loading and the unloading of the sensor, was 0.16 pF, which is $\sim 26\%$ of total range (0.58 pF) of the sensor. Although the sensor had hysteretic behavior, the mean line is linear. The hysteresis can be partly caused by geometric deformations in the sensor, as evident from the P - D curve (Fig. 6b inset).

The dynamic response of the sensor was studied by applying 12.5 kPa cyclic pressure on the sensor with a 0.2 Hz frequency and recording the relative C . Fig. 6c shows that when measuring the $C - C_0$ over a time window of ~ 2.5 hours (1800 cycles), there is an initial slow drift in the sensor response for the first ~ 1000 cycles, but the sensors then seem to stabilize. However, looking at shorter time windows, the behavior is relatively stable already before reaching 1000 cycles (Fig. 6c inset). The slow drift can be caused by the surfaces of the electrodes and dielectrics taking some cycles to settle since they are not perfectly planar.

To study the effect of aging of the sensor on its capacitance C , we fabricated a fresh sensor and measured the relative capacitance $C - C_0$ versus applied pressure P . We then redid the same measurements after the sensor had aged three and ten days. Fig. 6d shows that the relative $C - C_0$ slightly increases as the sensor ages, but the overall behavior of the sensor stays relatively similar. An increase in capacitance usually implies that the dielectric layer becomes thinner. Upon repeated usage and over a few ways, the adhesive material in the tape may have settled leading to a decrease in the thickness of the dielectric layer and change in the capacitance values.

Using the same data as in Fig. 6a, the sensitivity S of the sensor as a function of pressure P was calculated as

$$S = \frac{d(C)}{dP}, \quad (1)$$

where C is the capacitance, C_0 is the initial capacitance and P is applied pressure. The calculated sensitivity is shown in Fig. 6e. The maximum sensitivity was $4.5 \times 10^{-3} \text{ kPa}^{-1}$ and it was achieved with the smaller applied pressures. The sensitivity tends to decrease when the applied load was increased. This behavior can be beneficial for practical applications: the sensor has a high dynamic range.

As the main constituent of the electrode and the dielectric layer is cellulose and lignin, the sensor can be considered biodegradable. These materials can be easily degraded using enzymes such as cellulase and lacclase that are found in the many atmospheric bacteria and fungi [28], [29] In addition, Ag itself is not toxic to the environment and is biologically nonreactive compound during biological processes [30]. In the initial study, we stored the skeleton electrode in tap water and monitored the degradability for 150+ days (Fig. 6f). As evident from Fig. 6f, the leaf skeleton showed significant degradation. We conclude that the sensor is biodegradable and can be expected to be easily processable as waste.

Finally, the sensor was demonstrated in a throat movement capturing application (Fig. 7 and Video S1). The movements of the throat can indicate when the test person is breathing, speaking, or laughing even if there is no sound formed. This allows the tracking of speaking even if the person cannot speak or they must speak quietly. For the demonstration, the sensor was attached in the middle of the neck of the test person and the capacitance C was recorded while the test person was breathing normally, talking, and laughing. The sensor was able to capture a difference in the wave form of the signal when the test person was breathing (low peaks in the signal), talking (high peaks in the signal), and laughing (high and steep peaks in the signal).

This ability to capture different movements of the throat can be useful in future applications if speak capturing without a voice is needed.

IV. CONCLUSION

In conclusion, we fabricated biodegradable and transparent electrodes and used them to fabricate flexible and transparent tactile pressure sensors. The electrode and the sensor were characterized and found to be sensitive and capable to capture relatively low and high pressures. The sensor is also biodegradable and can be expected to produce very little e-waste. We noticed that there is hysteresis between the approach and the retraction curves, but the mean line is linear. Additionally, the sensors response was affected by the aging of the sensor. The sensor could be advantageous in applications where dynamic events are captured and single use sensors are needed: like in the medical field where the sensors need to be clean for every patient. Also, these sensors could be useful in the rural areas where there are no recycling systems and the sensors can be easily processed after use. Finally, we demonstrated our sensor in throat movement capturing application. Our sensor was able to capture breathing, speaking, and laughing movements.

ACKNOWLEDGMENT

A. Koivikko and V. Lampinen contributed equally. V. Sharma fabricated the leaf electrodes and took the SEM images. K. Yiannacou and V. Sharma did the electrode characterization experiments, A. Koivikko and V. Lampinen fabricated and characterized the sensor together with V. Sharma. A. Koivikko and V. Sharma wrote the paper together with the inputs from all the authors. V. Sariola. and V. Sharma conceived the research.

REFERENCES

- [1] X. Chen, J. A. Rogers, S. P. Lacour, W. Hu, and D.-H. Kim, "Materials chemistry in flexible electronics," *Chem. Soc. Rev.*, vol. 48, no. 6, pp. 1431–1433, 2019.
- [2] S. Huang, Y. Liu, Y. Zhao, Z. Ren, and C. F. Guo, "Flexible electronics: Stretchable electrodes and their future," *Adv. Funct. Mater.*, vol. 29, no. 6, p. 1805924, 2019.
- [3] D. Zhang, T. Huang, and L. Duan, "Emerging Self-Emissive Technologies for Flexible Displays," *Adv. Mater.*, vol. 32, no. 15, p. 1902391, 2020.
- [4] A. Elsayes, V. Sharma, K. Yiannacou, A. Koivikko, A. Rasheed, and V. Sariola, "Plant-Based Biodegradable Capacitive Tactile Pressure Sensor Using Flexible and Transparent Leaf Skeletons as Electrodes and Flower Petal as Dielectric Layer," *Adv. Sustain. Syst.*, p. 2000056, 2020.
- [5] J. Ramanujam *et al.*, "Flexible CIGS, CdTe and a-Si: H based thin film solar cells: A review," *Prog. Mater. Sci.*, vol. 110, p. 100619, 2020.
- [6] A. P. Gerratt, H. O. Michaud, and S. P. Lacour, "Elastomeric electronic skin for prosthetic tactile sensation," *Adv. Funct. Mater.*, vol. 25, no. 15, pp. 2287–2295, 2015.
- [7] V. Rantanen, P.-H. Niemenlehto, J. Verho, and J. Lekkala, "Capacitive facial movement detection for human–computer interaction to click by frowning and lifting eyebrows," *Med. Biol. Eng. Comput.*, vol. 48, no. 1, pp. 39–47, 2010.
- [8] D. Lee, G. Bang, M. Byun, and D. Choi, "Highly flexible, transparent and conductive ultrathin silver film heaters for wearable electronics applications," *Thin Solid Films*, vol. 697, p. 137835, 2020.
- [9] D. Li, W. Lai, Y. Zhang, and W. Huang, "Printable transparent conductive films for flexible electronics," *Adv. Mater.*, vol. 30, no. 10, p. 1704738, 2018.
- [10] Y. Khan, A. Thielens, S. Muin, J. Ting, C. Baumbauer, and A. C. Arias, "A New Frontier of Printed Electronics: Flexible Hybrid Electronics," *Adv. Mater.*, vol. 32, no. 15, p. 1905279, Apr. 2020.
- [11] A. K. Awasthi, J. Li, L. Koh, and O. A. Ogunseitan, "Circular economy and electronic waste," *Nat. Electron.*, vol. 2, no. 3, p. 86, 2019.
- [12] B. Yu *et al.*, "An elastic second skin," *Nat. Mater.*, vol. 15, no. 8, p. 911, 2016.
- [13] X. Wang, L. Dong, H. Zhang, R. Yu, C. Pan, and Z. L. Wang, "Recent progress in electronic skin," *Adv. Sci.*, vol. 2, no. 10, p. 1500169, 2015.
- [14] A. Atalay *et al.*, "Batch fabrication of customizable silicone-textile composite capacitive strain sensors for human motion tracking," *Adv. Mater. Technol.*, vol. 2, no. 9, p. 1700136, 2017.
- [15] D. P. J. Cotton, I. M. Graz, and S. P. Lacour, "A multifunctional capacitive sensor for stretchable electronic skins," *IEEE Sens. J.*, vol. 9, no. 12, pp. 2008–2009, 2009.
- [16] Q. Fu, Y. Chen, and M. Sorieul, "Wood-Based Flexible Electronics," *ACS Nano*, vol. 14, no. 3, pp. 3528–3538, 2020.
- [17] D. Zhao, Y. Zhu, W. Cheng, W. Chen, Y. Wu, and H. Yu, "Cellulose-Based Flexible Functional Materials for Emerging Intelligent Electronics," *Adv. Mater.*, p. 2000619, 2020.
- [18] V. R. Feig, H. Tran, and Z. Bao, "Biodegradable Polymeric Materials in Degradable Electronic Devices," *ACS Cent. Sci.*, vol. 4, no. 3, pp. 337–348, Mar. 2018.
- [19] D. Sinar and G. K. Knopf, "Disposable piezoelectric vibration sensors with PDMS/ZnO transducers on printed graphene-cellulose electrodes," *Sensors Actuators A Phys.*, vol. 302, p. 111800, 2020.
- [20] H. Koga and M. Nogi, "Cellulose Paper Composites for Flexible Electronics," in *Lignocellulosics*, Elsevier, 2020, pp. 171–191.
- [21] V. Sharma, A. Koivikko, K. Yiannacou, K. Lahtonen, and V. Sariola, "Flexible biodegradable transparent heaters based on fractal-like leaf skeletons," *npj Flex. Electron.*, vol. 4, no. 1, 2020.
- [22] W. Wu, R. M. Guijt, Y. E. Silina, M. Koch, and A. Manz, "Plant leaves as templates for soft lithography," *RSC Adv.*, vol. 6, no. 27, pp. 22469–22475, 2016.
- [23] Y. J. Fan *et al.*, "Highly Robust, Transparent, and Breathable Epidermal Electrode," *ACS Nano*, vol. 12, no. 9, pp. 9326–9332, 2018.
- [24] R. F. Shepherd *et al.*, "Multigait soft robot," *Proc. Natl. Acad. Sci. U. S. A.*, vol. 108, no. 51, pp. 20400–20403, 2011.
- [25] R. V. Martinez *et al.*, "Robotic tentacles with three-dimensional mobility based on flexible elastomers," *Adv. Mater.*, vol. 25, no. 2, pp. 205–212, 2013.
- [26] A. Elsayes, V. Sharma, K. Yiannacou, A. Koivikko, A. Rasheed, and V. Sariola, "Plant-Based Biodegradable Capacitive Tactile Pressure Sensor Using Flexible and Transparent Leaf Skeletons as Electrodes and Flower Petal as Dielectric Layer," *Adv. Sustain. Syst.*, vol. 4, no. 9, 2020.
- [27] S. R. A. Ruth, L. Beker, H. Tran, V. R. Feig, N. Matsuhisa, and Z. Bao, "Rational Design of Capacitive Pressure Sensors Based on Pyramidal Microstructures for Specialized Monitoring of Biosignals," *Adv. Funct. Mater.*, vol. 30, no. 29, pp. 1–12, 2020.
- [28] J. Simon, H. P. Müller, R. Koch, and V. Müller, "Thermoplastic and biodegradable polymers of cellulose," *Polym. Degrad. Stab.*, vol. 59, no. 1–3, pp. 107–115, 1998.
- [29] G. Janusz, A. Pawlik, J. Sulej, U. Świdarska-Burek, A. Jarosz-Wilkolazka, and A. Paszczyński, "Lignin degradation: Microorganisms, enzymes involved, genomes analysis and evolution," *FEMS Microbiol. Rev.*, vol. 41, no. 6, pp. 941–962, 2017.
- [30] H. T. Ratte, "Bioaccumulation and toxicity of silver compounds: A review," *Environ. Toxicol. Chem.*, vol. 18, no. 1, pp. 89–108, Jan. 1999.



Anastasia Koivikko received the B.Sc. and M.Sc. degrees in biomedical engineering from the Tampere University of Technology, Tampere, Finland, in 2015 and 2017, respectively, where she is currently pursuing the D.Sc. degree. In 2019, she worked a guest researcher in Max Planck Institute for Intelligent Systems. Her research interests include fabrication of soft robots, especially soft grippers, and integration of stretchable sensors into soft robotic systems.



Vilma Lampinen received the B.Sc. degree in biomedical engineering from the Tampere University, Tampere, Finland, in 2020. Alongside of her master's studies in biomedical engineering, she has been working in a research group in the field of bioinspired materials and robotics.



Kyriacos Yiannacou received his B.Sc. in Electrical Engineering in 2016 from Frederick University, Nicosia, Cyprus, and in 2019 his M.Sc. degree in Automation science and Engineering from the Tampere University, Tampere, Finland. Since then he is pursuing the Ph.D. degree. His research interests include manipulation methods in acoustic microfluidics.



Vipul Sharma received Ph.D. degree in Nanotechnology from the Indian Institute of Technology Mandi, India in 2018. Previously, he received his M.Tech. degree in Nanoscience and Nanotechnology from Amity University, India in 2012. He joined Tampere University as a postdoctoral researcher under the supervision of Dr. Veikko Sariola in 2018. He was awarded the Academy of Finland postdoctoral fellowship in 2020. He has authored and co-authored 35 international journal and conference articles in the field of nanotechnology, bioinspiration/biomimetics, and flexible electronics. His research interests include design, fabrication, and characterization of bioinspired and biomimetic functional surfaces, flexible electronics, nanofabrication, plasmonic nanoparticles, semiconductor nanoparticles, biodegradable polymers, and bioinspired materials.



Veikko Sariola (M'17) received the D.Sc. (Tech.) degree in electrical engineering from Aalto University, Finland, in 2012. From 2013 to 2015, he was a Post-Doctoral Researcher with Carnegie Mellon University. In 2016, he was appointed as a Research Fellow by the Academy of Finland. He is currently an Associate Professor of Biomedical Microsystems with the Tampere University, Finland. His current research interests include bio-inspired materials and robotics.